Available online at www.sciencedirect.com

ScienceDirect

Procedia CIRP 88 (2020) 467–472

www.elsevier.com/locate/procedia

13th CIRP Conference on Intelligent Computation in Manufacturing Engineering, CIRP ICME '19

Ultrasonic evaluation of induction heat treatment applied to thermoplastic matrix CFRP

Tiziana Segreto[a,b,*], Alberto Bottillo[a,b], Barbara Palmieri[b], Luigi Nele[b], Roberto Teti[a,b]

[a]*Fraunhofer Joint Laboratory of Excellence on Advanced Production Technology (Fh-J_LEAPT UniNaples), Naples, Italy*
[b]*Dept. of of Chemical, Materials and Industrial Production Engineering, University of Naples Federico II, P.le Tecchio 80, 80125 Naples, Italy*

* Corresponding author. Tel.: +39-081-7682371; fax: +39-081-7682362. E-mail address: tsegreto@unina.it

Abstract

Thermoplastic matrix carbon fibre reinforced polymers (CFRP) are extensively utilized for composites structures in the aerospace and aeronautical industries. Diverse techniques were currently applied to joining composite parts, the most promising method is the induction heat treatment. In this paper, experimental tests were performed on thermoplastic matrix CFRP specimens by varying the induction heat treatment parameters: power, frequency and current. An advanced ultrasonic (UT) non-destructive evaluation based on pulse-echo technique was employed for the investigation of the utilized process parameters through the UT evaluation of the process induced damage and its depth along the thickness of the thermoplastic matrix CFRP laminates.

Keywords: Thermoplastic matrix CFRP; Induction heat treatment; Ultrasonic non-destructive evaluation

1. Introduction

Nowadays, the use of carbon fibre reinforced polymer (CFRP) thermoplastic composites in the aerospace industry is increasing due to their better damage tolerance properties than thermosetting ones [1]. Moreover, thermoplastic composites offer the possibility to be joined by welding. Joining by welding avoid problems related to mechanical fastening as possible delamination and stress concentrations [2, 3] as well as long curing time and the need for extensive surface preparation linked to adhesive bonding [4].

Welding allows joining two or more parts by fusing their contact interfaces. The most promising techniques for joining high-performance thermoplastic composites for aerospace applications are resistance, ultrasonic and electromagnetic induction welding [5, 6]. All these processes permit to obtain an efficient production of heat by an external energy source.

Induction welding is considered to have the highest potential due to the rapid rate of heating and the ease of automation. This technique is based on eddy currents induced in a ferromagnetic or conductive material placed close to an alternating magnetic field with a frequency range between kHz and MHz. Thermoplastic composites cannot be heated by electromagnetic induction because they are neither electromagnetic nor electrically conductive. A susceptor, such as particles, metallic or carbon fibre fabric, may be used [7]. Thermoplastic matrix CFRP may be heated directly due to the presence of electrically conductive carbon fibres, but only as fabric reinforcement. The fundamental condition for the generation of eddy currents is the formation of closed electrical loops [8, 9].

The main parameters that characterise induction heating of thermoplastic matrix CFRP are: coil geometry, applied electrical power, and coil current; moreover, the frequency and the coupling distance play a key role.

Until now, the attention of researchers has been dedicated to study the role of parameters such as heating time, pressure and temperature and never the frequency [10, 11].

The frequency is a fundamental parameter, since from it depend the characteristics of the generated alternating magnetic field, and consequently, the eddy currents induced in the material. The frequency influences the heat penetration depth:

10.1016/j.procir.2020.05.081

keeping constant the current, a higher frequency results in more power in the workpiece and faster heating of composites [8]; but, high frequencies limit the penetration depth of the electromagnetic field due to the "skin effect" [12]. For metal alloys, the heating depth of penetration can be obtained by Maxwell's equations, the formula of which is as follows:

$$\delta = \sqrt{(\rho/(\pi * \mu * f))} \quad (1)$$

where ρ is the material resistivity, μ is the magnetic permeability and f is the frequency.

In this paper, diverse experimental tests were conducted by varying the induction heat treatment parameters: power, frequency and current. The power level is keeping almost constant giving iso-power conditions whereas the frequency and current are variable for each selected power level.

The aim of this paper is to evaluate the role of the induction heat treatment parameters (power, frequency and current) through the ultrasonic evaluation of the process induced damage and its depth along the thickness of thermoplastic matrix CFRP laminates.

For this reason, an ultrasonic (UT) non-destructive evaluation (NDE) technique based on full volume (FV) ultrasonic scanning [13 - 16] was applied to thermoplastic matrix CFRP specimens in order to generate UT images of the internal material structure of the laminates. The evaluation of the induction heat treatment was achieved through the analysis of the generated multiple UT images. Moreover, a metrological analysis was carried out in order to identify the process induced damage depth in the CFRP thickness direction.

2. Materials and methods

The utilized materials were provided by TenCate advanced composites (TenCate Cetex) consisting of Polyphenylene sulfide (PPS) semicrystalline matrix and a T300 Carbon fabric, with a volume fraction of 50%. The carbon fibre PPS laminates are composed of 8 plies arranged according to $[0°/90]_{4s}$ and have a thickness of 2.5 mm. Squared specimens of 40 mm x 40 mm size were cut from the manufactured laminates and were subjected to an induction heat treatment (Fig. 1).

The experimental tests were carried out using an Egma 30R generator designed and developed by Felmi (Italy). The power can be tuned to 30 kW ranging from 20% to 100%. The frequency range can vary only changing the coil geometry. The shape of the adopted coil was chosen after a study on the edge effect [17, 18] with the aim to obtain a uniform temperature distribution on the surface. Figure 2 shows the coil geometry realised to obtain the frequency of 150 kHz: the coil has an external diameter of 24 mm, while the diameter of the utilized copper tube is 4 mm with 2 mm of thickness.

The experimental set-up using a 200 kHz coil was shown in Figure 3 and was characterised by a heating unit including a "circular" coil and a ceramic support. The coil was not in contact with the composite laminate, but it is at a fixed distance of 2 mm from the specimen's surface.

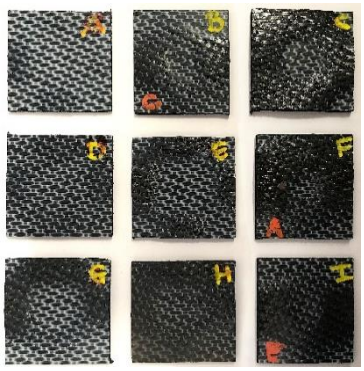

Fig. 1. Induction heat treatment of thermoplastic matrix CFRP specimens.

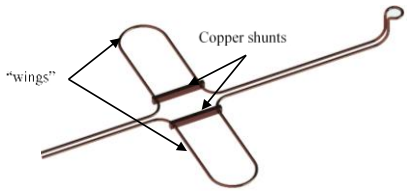

Figure 2: Coil geometry for the frequency of 150 kHz with copper shunts.

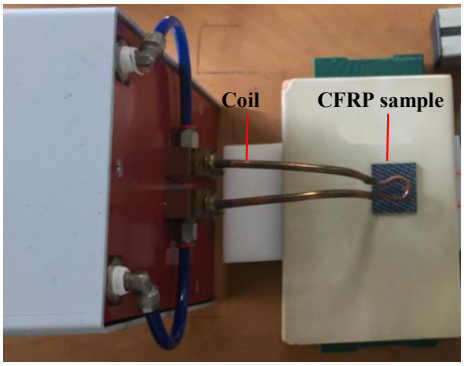

Figure 3: Experimental set-up for the induction heat treatment on thermoplastic matrix CFRP with the 200 kHz coil.

A generator controls the frequency by an automatic coupling system called "auto-tuning system", but the only way to vary the frequency is to change of the geometry and the size of the coil. The frequency at which the generator oscillates is that of resonance between the inductance of the connected coil and the capacitance of the capacitor placed inside the generator. The formula to apply is:

$$f = \frac{1}{2\pi\sqrt{LC}} \quad (2)$$

where L is the inductance and C is the capacitance.

The high-frequency alternate current in the coil produced a time-variable magnetic field of the same frequency in near surroundings, which then induced eddy currents in the composite laminate to be heated.

The alternating magnetic field induced a voltage, V, in a conductive fibre loop is defined as [8]:

$$V = 2\pi * f * \mu * H * A \quad (3)$$

where f is the frequency, H is the magnetic field intensity, μ is

the magnetic permeability, and A is the area.

The value of the inductance depends on the geometrical features of the coil such as length l, the section A of the spire, the number of turns N (span density n = N / l); moreover, by keeping the geometry constant, the way to change the frequency, is varying the total length of the coil.

The induction heating experiments were performed with different values of the frequency: 130 kHz, 150 kHz and 200 kHz in order to highlight the effect of the frequency on the heating depth penetration.

As stated above, to obtain a frequency of 200 kHz, the coil has a length of 200 mm, as shown in Figure 3. Conversely, to obtain a frequency of 130 kHz and 150 kHz was used the coil shown in Figure 2, with the same geometry of the coil at 200 kHz, but with a total length of 500 mm and of 300 mm, respectively. The length of 300 mm was obtained by inserting two copper shunts in the "two wings", thus reducing the total length of the coil and allow to change the final frequency.

The actual frequency set, varying the coils, was verified by the machine display used for the experimental tests. The display shows the operating parameters of the machine, such as coil current and frequency.

Finally, nine induction heat treatment tests were performed by varying the frequency and current values in an iso-power regime (power level = 97 W, 135 W and 162 W) as summarized in Table 1. In particular, the frequency values increase when the current values decrease and vice versa according to the following equation:

$$P = \frac{V^2}{R_f} = \frac{4\pi^2 \cdot f^2 \cdot \mu^2 \cdot H^2 \cdot A^2}{R_f} \quad (4)$$

where R_f is the electrical resistance of the carbon fibres. Furthermore, the magnetic field intensity H is given by:

$$H = \frac{i}{4\pi} \cdot \int \frac{1}{|\vec{r}|^2} \cdot \left| d\vec{l} \times \left(\frac{\vec{r}}{|\vec{r}|}\right) \right| \quad (5)$$

where *i* is the coil current, *dl* a section of the coil length, and r is the distance between the coil and some point P [8]. According to Eq. 4 and 5, P is also proportional to the current squared.

3. Ultrasonic (UT) non-destructive evaluation (NDE)

3.1. UT NDE system

The system utilized for the ultrasonic non-destructive evaluation of the induction heat treatment applied to the thermoplastic matrix CFRP specimens is developed at Fh-J_LEAPT UniNaples, Italy [19]. This UT NDE system is based on the employment of a 6-axis robotic arm for the UT probe displacement. An oscillator/detector is utilized for the UT probe excitation and the detection of the UT returning signals which are sent to a digital oscilloscope for their acquisition, visualization and digitization. A custom made software allows the UT waveform acquisition and processing as well as the control of the robotic arm for probe displacement [18-20].

Table 1. Induction heat treatment parameters for the experimental tests.

Power level [W]	Frequency [KHz]	Current [A]	Specimen ID
97	130	15	A
	150	13	B
	200	10	C
135	130	22	D
	150	20	E
	200	15	F
162	130	27	G
	150	25	H
	200	20	I

3.2. Pulse-echo UT scanning tests

A pulse-echo UT technique [21- 23] was utilized for the detection of the complete UT waveform (full volume – FV) for each probe position in the x-y raster scanning of the CFRP specimens as shown in Figure 4.

The FV UT scans were executed in water by positioning the CFRP specimens with not treated surface as front surface (Figure 5).

A focused high frequency (15 MHz) UT probe with focal length of 5.09 mm was used as immersion probe. The oscillator/detector was set at 90 dB gain and medium damping whereas the digital oscilloscope was set at 1 V (Volts/div), 0.5 µs (Time/div) and 100 MHz sampling frequency, achieving 500 samplings for each detected UT waveform.

The UT scanning area was equal to 30 mm x 30 mm with a scan step of 0.3 mm. After each scan, the obtained UT data were stored in a volumetric file containing the entire set of digitized UT waveforms for each material x-y interrogation point.

3.3. UT images generation

The UT data files were pre-processed using a custom made software in order to generate single or multiple UT images that highlight the internal structure of the thermoplastic matrix CFRP specimen under investigation.

This pre-processing phase consists of two main steps:

1. Selection of the typical UT waveform from the volumetric data file obtained for the specific thermoplastic matrix CFRP specimen. This typical UT waveform is a diagram (Figure 6) having the time-of-flight (in seconds) as x axis and the UT signal as y axis (in Volt/div). The time-of-flight (ToF) is the time taken by the UT signal to traverse the complete composite thickness back and forth.
2. Time axis subdivision: two red lines were utilized to define the portion of the UT signal to be subdivided. The possible UT equal subdivisions ranged from 1 (corresponding to a single UT image) to 16 for multiple UT images generation. As the time axis represents the UT travel in the thickness direction of the specimen, each subdivision (sub-gate width) represents the internal material structure of the corresponding thickness portion of the thermoplastic matrix CFRP specimen.

For each of the 9 thermoplastic matrix CFRP specimens, the time gate subdivisions were fixed equal to 16.

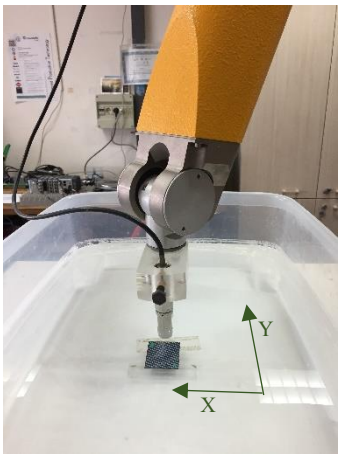

Fig. 4. Pulse-echo FV-UT scans of thermoplastic matrix CFRP specimen.

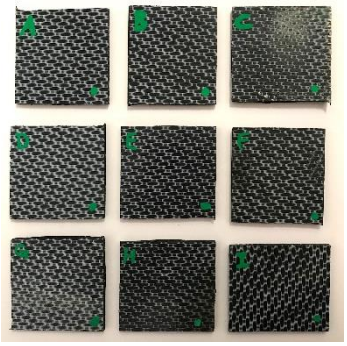

Fig. 5. Thermoplastic matrix CFRP specimens: ultrasonic inspection side.

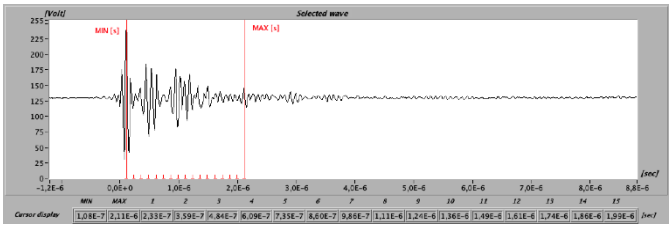

Fig.6. Typical UT waveform for the thermoplastic matrix CFRP specimen.

3.4. UT image analysis results

For the UT non-destructive evaluation of the induction heat treatment, the generated 16 UT images for each of 9 thermoplastic matrix CFRP specimens were analysed. The 16 equal subdivisions of the UT signals correspond to 1/16 of the CFRP specimen thickness, i.e. about 0. 16 mm.

Figures 7 - 10 show the 16 UT images obtained for the A, B, C, G thermoplastic matrix CFRP specimens arranged in succession from left to right and from top to bottom and relates to 0.16 mm of the laminate nominal thickness. Each thermoplastic matrix CFRP specimen was scanned on the not heat treated surface, therefore the first UT image corresponds to the 2.50 mm - 2.34 mm thickness portion of the CFRP sample, the second UT image corresponds to the 2.34 mm - 2.19 mm thickness portion of the sample, and so on, up to the last UT image corresponding to the first laminate thickness portion ranging from 0.16 to 0 mm (induction heat treatment start).

As regards the A thermoplastic matrix CFRP specimen with induction heat treatment parameters equal to 97 W, 130 KHz, and 15 A, from Figure 7 it can be noticed that the process induced damage is present starting from the 5th UT image whereas in the first four UT images no induced damage is highlighted.

The B and C thermoplastic matrix CFRP specimens are subjected to an induction heat treatment with the same power level of the A CFRP specimen (97 W) but with diverse frequency and current values. Figures 8 and 9 show that the induced process damage is clearly visible in the 2nd UT image but it is not evident in the 1st UT image for both the B and C laminate. Moreover, the UT images reveal that the induced process damage develops differently for the sample B and C. In particular, for the B specimen, the induce damage develops also at the center of the laminate making difficult to recognize the fiber orientation whereas for the C specimen the induce damage permits to identify the fiber orientations for each layer.

As regards the G thermoplastic matrix CFRP specimen with power level (162 W) higher than the A sample but having the same frequency value of 130 KHz, the UT images (Figure 10) show that the process induced damage covers almost the whole sample area, unlike what happens with laminate A.

3.5. Estimation of the process induced damage depth

A metrological analysis was performed in order to estimate the depth of the process induced damage along the composites thickness using the following formula:

$$v = \frac{s}{\Delta T/2} \tag{6}$$

where s is the nominal thickness of the thermoplastic matrix CFRP composite, v is the UT velocity in the CFRP composite and ΔT is the time-of-flight.

After the 16 UT images generation and analysis, each image representing the induced damage end (e.g. the 5th UT image for the A specimen) was analyzed once again by using a dedicated time gate subdivision generating new UT images revealing the presence of the damage in a precise ΔT.

By using the formula 6, it is possible to calculate the depth of the process induced damage using the known ΔT and the UT velocity. Table 2 summarized the calculated end depth of the induced process damage along the thickness direction for each CFRP specimen.

Table 2. Induced process damage depth.

Specimen ID	Induced process damage depth
A	~ 1.80 mm
B	~ 2.36 mm
C	~ 2.42 mm
D	~ 2.03 mm
E	~ 2.38 mm
F	Cover the entire sample
G	~ 2.26 mm
H	Cover the entire sample
I	Cover the entire sample

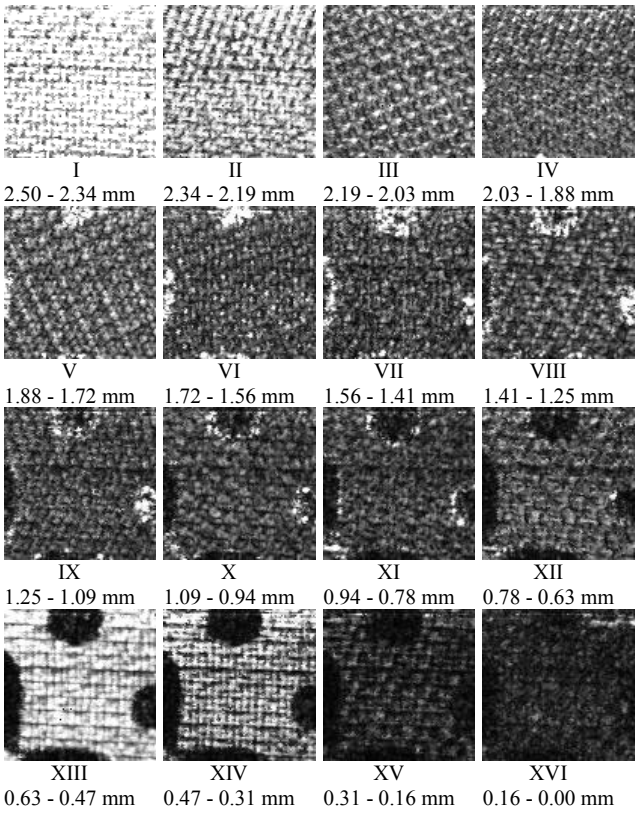

Fig. 7. Sixteen UT images of the A thermoplastic matrix CFRP specimen. Each UT image relates to 1/16 of the component nominal thickness.

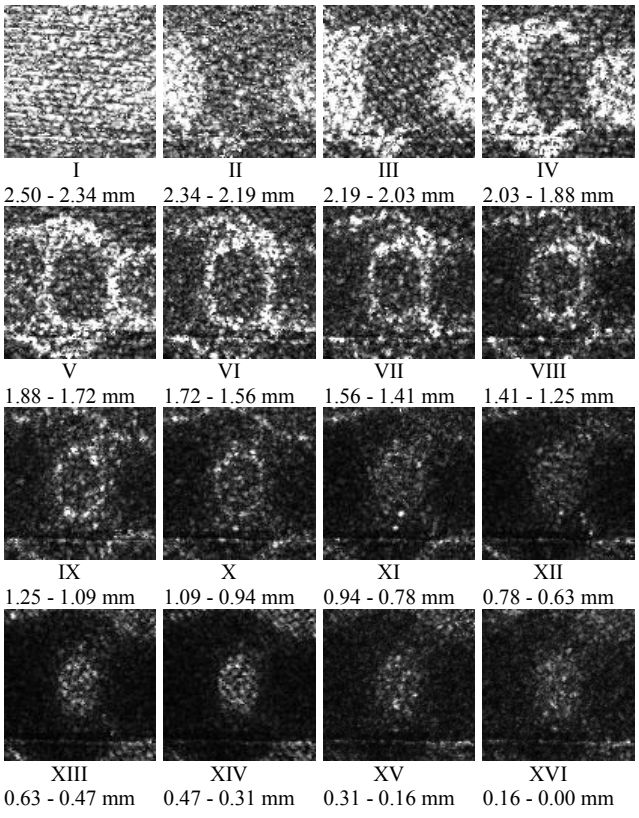

Fig. 8. Sixteen UT images of the B thermoplastic matrix CFRP specimen. Each UT image relates to 1/16 of the component nominal thickness.

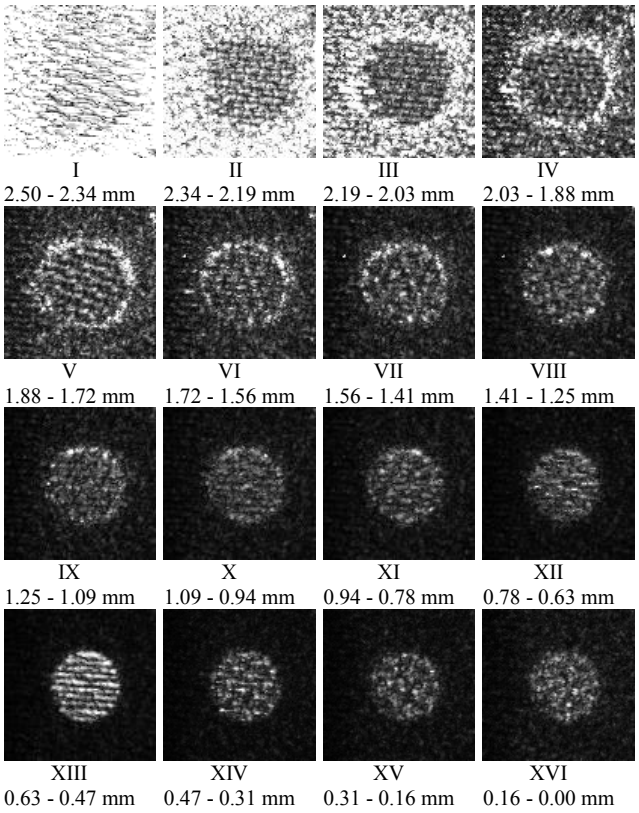

Fig. 9. Sixteen UT images of the C thermoplastic matrix CFRP specimen. Each UT image relates to 1/16 of the component nominal thickness.

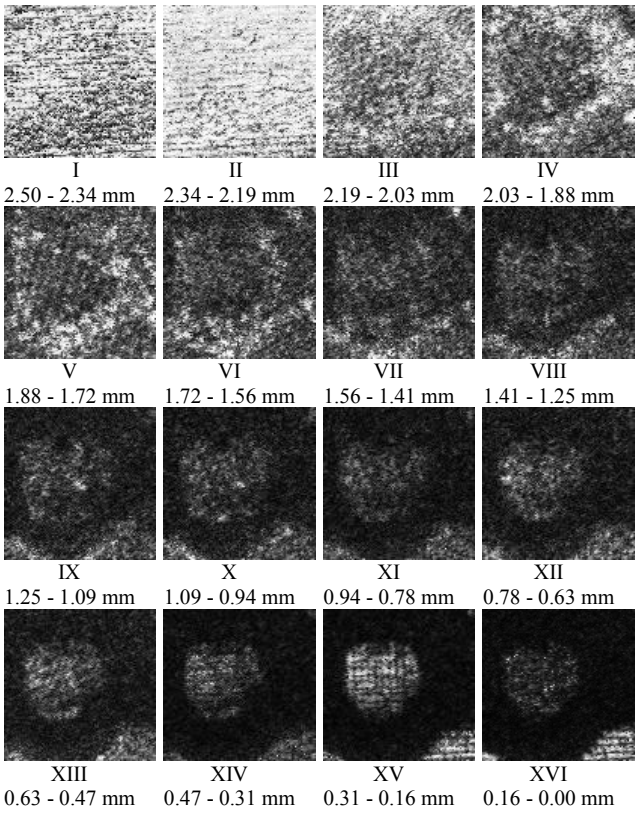

Fig. 10. Sixteen UT images of the G thermoplastic matrix CFRP specimen. Each UT image relates to 1/16 of the component nominal thickness.

By combining the results obtained from the UT image analysis and the estimation of the depth of the process induced damage for each of the 9 thermoplastic matrix CFRP specimens, it can be noticed that the frequency values influenced the damage development during a heat induction process. In particular, for higher values of the frequency, the magnetic field penetrates more deeply, and consequently, the distribution of heat within the CFRP specimen is more uniform and, keeping constant the power, the composite tends to heat up faster.

4. Conclusions

An advanced UT NDE system was utilized for the evaluation of induction heat treatment applied to thermoplastic matrix CFRP specimens through the identification of the process induced damage and its depth along the thickness of the laminates.

Diverse experimental tests were performed by varying the induction heat treatment parameters: power, frequency and current. The evaluation of the role of the utilized induction heat treatment parameters was carried out through an analysis of the obtained UT images for each thermoplastic matrix CFRP specimens.

The UT NDE results showed that the utilized frequency values play a key role during the induction heat treatment. In particular, when a same power level was used, the higher the frequency, the higher the heat penetration in the material thickness. On the contrary, the lower the frequency, the lower the heat penetration. For higher values of the frequency less power is needed to reach the target temperature of the defined point, since the time to reach the target temperature is less than in the case of lower frequency case.

As future developments, a new experimental campaign will be carried out with different process parameters and an analysis on further set-up (e.g. coupling distance between coil and laminate, dimension of the coil) will be performed.

Acknowledgements

The Fraunhofer Joint Laboratory of Excellence on Advanced Production Technology (Fh-J_LEAPT UniNaples) is gratefully acknowledged for its support to this research.

References

[1] Harper CA. Handbook of plastics, elastomers, and composites. McGraw-Hill; 2002.
[2] Haque R, Durandet Y. Strength prediction of self-pierce riveted joint in cross-tension and lap-shear. Mater Des 2016;108:666-78.
[3] Angelone R, Caggiano A, Improta I, Nele L. Characterization of hole quality and temperature in drilling of Al/CFRP stacks under different process condition. Procedia CIRP 2019;79:319-24.
[4] Fotsing ER, Miron F, Eury Y, Ross A, Ruiz E. Bonding analysis of carbon/epoxy composites with viscoelastic acrylic adhesive. Compos Part B Eng 2012;43:2087-93.
[5] Stokes V. Joining methods for plastics and plastic composites: an overview. Polym Eng Sci 1989.
[6] Ageorges C, Ye L, Hou M. Advances in fusion bonding techniques for joining thermoplastic matrix composites: a review. Compos Part A Appl Sci Manuf 2001;32:839-57.
[7] Ahmed TJ, Stavrov D, Bersee HEN, Beukers A. Induction welding of thermoplastic composites—an overview. Compos Part A Appl Sci Manuf 2006;37:1638-51.
[8] Rudolf R, Mitschang P, Neitzel M. Induction heating of continuous carbon-fibre-reinforced thermoplastics. Compos Part A Appl Sci Manuf 2000;31:1191-202.
[9] Fink BK, McCullough RL, Gillespie Jr. JW. Induction Heating of Carbon-Fiber Composites : Electrical Potential Distribution Model 1999:45.
[10] Ahmed TJ, Stavrov D, Bersee HEN, Beukers A. Induction welding of thermoplastic composites—an overview. Compos Part A Appl Sci Manuf 2006;37:1638-1651.
[11] Banik N. A review on the use of thermoplastic composites and their effects in induction welding method. Materials Today: Proceedings 2018;5/9: 20239-20249.
[12] Moser L. Experimental analysis and modeling of susceptorless induction welding of high performance thermoplastic polymer composites. Inst. für Verbundwerkstoffe; 2012.
[13] Chaplin R. Industrial Ultrasonic Inspection: Levels 1 and 2. FriesenPress, Canada; 2017. p. 292.
[14] Gholizadeh S. A review of non-destructive testing methods of composite materials. Procedia Structural Integrity 2016;1:50-57.
[15] Hassen AA, Taheri H, Vaidya UK. Non-destructive investigation of thermoplastic reinforced composites. Composites Part B: Engineering 2016;97:244-254
[16] Langenberg KJ, Marklein R, Mayer K. Ultrasonic nondestructive testing of materials: theoretical foundations. CRC Press; 2012.
[17] A.K. Miller, C. Chang, A. Payne, M. Gur, E. Menzel AP. The nature of induction heating in graphite–fiber, polymer–matrix composite materials. SAMPE J 1990;26:37-54.
[18] Palmieri B, Nele L, Galise F. Numerical modeling and experimental validation of thermoplastic composites induction welding. AIP Conf. Proc. 2018, p. 050013.
[19] http://www.jleapt-unina.fraunhofer.it/
[20] Segreto T, Teti R and Lopresto V. Non-destructive testing of low-velocity impacted composite material laminates through ultrasonic inspection methods. In: Characterizations of some composite materials. IntechOpen, 2018. DOI: 10.5772/intechopen.80573.
[21] Segreto T, Bottillo A, Caggiano A, Teti R, Ricci F. Full-volume ultrasonic technique for 3D thickness reconstruction of CFRP aeronautical components, Procedia CIRP 2018;67:434-439.
[22] Segreto T, Bottillo A, Caggiano A, Martorelli M. Integration of reverse engineering and ultrasonic non-contact testing procedures for quality assessment of CFRP aeronautical components, Procedia CIRP 2019;79:343-348.
[23] Segreto T, Bottillo A, Teti R. Advanced ultrasonic non-destructive evaluation for metrological analysis and quality assessment of impact damaged non-crimp fabric composites. Procedia CIRP 2016;41:1055-1060.